Journal of Hazardous Materials 460 (2023) 132348

Contents lists available at ScienceDirect

Journal of Hazardous Materials

journal homepage: www.elsevier.com/locate/jhazmat

Realism-based assessment of the efficacy of potassium peroxymonosulphate on *Stenotrophomonas maltophilia* biofilm control

Isabel M. Oliveira [a,b], Inês B. Gomes [a,b], Tânia Moniz [c,d], Lúcia Chaves Simões [e,f], Maria Rangel [d], Manuel Simões [a,b,*]

[a] LEPABE – Laboratory for Process Engineering, Environment, Biotechnology and Energy, Faculty of Engineering, University of Porto, Rua Dr Roberto Frias, 4200-465 Porto, Portugal
[b] ALiCE – Associate Laboratory in Chemical Engineering, Faculty of Engineering, University of Porto, Rua Dr Roberto Frias, 4200-465 Porto, Portugal
[c] REQUIMTE, LAQV – Department of Chemistry and Biochemistry, Faculty of Sciences, University of Porto, Rua do Campo Alegre, s/n, 40169-007 Porto, Portugal
[d] REQUIMTE, LAQV – Instituto de Ciências Biomédicas de Abel Salazar, University of Porto, Rua de Jorge Viterbo de Ferreira, 228, 4050-313 Porto, Portugal
[e] CEB – Centre of Biological Engineering, University of Minho, Campus de Gualtar, 4710-057 Braga, Portugal
[f] LABBELS – Associate Laboratory in Biotechnology, Bioengineering and Microelectromechanical Systems, Braga/Guimarães, Portugal

HIGHLIGHTS

- OXONE was effective against mature biofilms formed under simulated DW conditions.
- Chlorine only caused 1 log reduction in biofilm culturable and non-damaged cells.
- OXONE allowed great reduction of biofilm culturable and non-damaged cells.
- OXONE was more stable in synthetic tap water than chlorine.
- Presence of ROS during OXONE disinfection, particularly singlet oxygen.

GRAPHICAL ABSTRACT

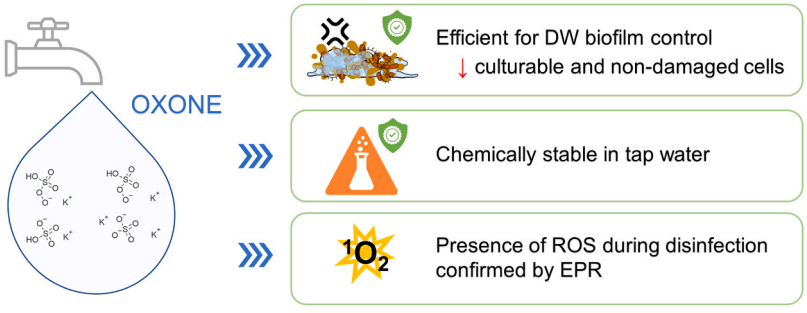

ARTICLE INFO

Editor: Jörg Rinklebe

Keywords:
Biofilm
Chemical stability
Disinfection
Drinking water
Pentapotassium bis(peroxymonosulphate) bis (sulphate) (OXONE)
Stenotrophomonas maltophilia

ABSTRACT

The potential of pentapotassium bis(peroxymonosulphate) bis(sulphate) (OXONE) to control biofilms in drinking water distribution systems (DWDS) was evaluated and compared to chlorine disinfection. Mature biofilms of drinking water (DW)-isolated *Stenotrophomonas maltophilia* were formed using a simulated DWDS with a rotating cylinder reactor (RCR). After 30 min of exposure, OXONE at 10 × minimum bactericidal concentration (MBC) caused a significant 4 log reduction of biofilm culturability in comparison to the unexposed biofilms and a decrease in the number of non-damaged cells below the detection limit (4.8 log cells/cm^2). The effects of free chlorine were restricted to approximately 1 log reduction in both biofilm culturability and non-damaged cells. OXONE in synthetic tap water (STW) at 25 ºC was more stable over 40 days than free chlorine in the same conditions. OXONE solution exhibited a disinfectant decrease of about 10% of the initial concentration during the first 9 days, and after this time the values remained stable. Whereas possible reaction of chlorine with inorganic and organic substances in STW contributed to free chlorine depletion of approximately 48% of the initial concentration. Electron paramagnetic resonance (EPR) spectroscopy studies confirmed the presence of

* Corresponding author at: LEPABE – Laboratory for Process Engineering, Environment, Biotechnology and Energy, Faculty of Engineering, University of Porto, Rua Dr Roberto Frias, 4200-465 Porto, Portugal.
E-mail address: mvs@fe.up.pt (M. Simões).

https://doi.org/10.1016/j.jhazmat.2023.132348
Received 30 May 2023; Received in revised form 4 August 2023; Accepted 17 August 2023
Available online 19 August 2023

singlet oxygen and other free radicals during *S. maltophilia* disinfection with OXONE. Overall, OXONE constitutes a relevant alternative to conventional DW disinfection for effective biofilm control in DWDS.

1. Introduction

In 2010, the United Nations General Assembly recognized access to safe drinking water (DW) as a basic Human right [1]. Given its importance as a health and development issue, efforts have been done to increase the number of people with access to safely managed DW services. According to the World Health Organization (WHO) and the United Nations Children's Fund (UNICEF) Joint Monitoring Programme for Water Supply, Sanitation and Hygiene (JMP), in 2020 the proportion of the global population using safely managed services accounted for 74%, estimating an increase to 81% coverage by 2030 at current rates of progress [2]. However, compliance with international guidelines for DW quality does not guarantee the prevention of biofilm development in DWDS. Biofilms are composed of cells embedded in extracellular polymeric substances (EPS) that protect microorganisms from disinfection and facilitate the recovery of injured cells [3,4]. The presence of biofilms in DWDS constitutes a public health risk given the higher tolerance to disinfection in comparison to the planktonic cell state [5-7], particularly if pathogens are inhabiting the biofilm community. Despite the application of conventional DW disinfection, different studies have been demonstrating the presence of opportunistic pathogens (*i.e. Legionella* spp., *Mycobacterium* spp., *Pseudomonas aeruginosa*, *Acanthamoeba* spp., and *Aeromonas* spp.) within the microbial communities of DW biofilms [8-10]. The elimination of biofilms in water networks is almost impossible to achieve and, to date, no approach has shown complete success in eradicating them [3,4]. Therefore, biofilm prevention and control in DWDS constitute a challenge to DW suppliers. The main strategy that has been broadly applied relies on a balance between nutrient removal from water and the presence of a residual disinfectant. Chlorine is the most commonly used disinfectant for water treatment and to control microbial accumulation in pipes and tanks [4,11]. However, it is incapable of the complete prevention of biofilm growth [12] and, if a chlorine decay is observed to sub-inhibitory concentrations, it can cause selective pressure to enrich antibiotic-resistant bacteria in biofilms [13, 14]. The maintenance of chlorine residual is negatively impacted by the water age, the presence of organic substances, pipe corrosion events, and an increase in water temperature [15-17]. Additionally, the formation of harmful disinfection by-products (DBP), such as trihalomethanes and haloacetic acids, has also highlighted the importance of finding new alternatives to conventional chlorination [18,19].

Currently, potassium peroxymonosulphate (also known as pentapotassium bis(peroxymonosulphate) bis(sulphate) or OXONE) is being evaluated by the European Chemicals Agency (ECHA) for disinfection of DW, and its initial application for approval is under opinion development by the Biocidal Products Committee [20]. OXONE is a chlorine-free oxidizing agent that has been broadly studied in the field of advanced oxidation processes for the decomposition of organic pollutants in wastewater or groundwater [21,22]. For instance, activated-peroxymonosulphate demonstrated to be effective for the degradation of ofloxacin [23], sulfamethazine [24], sulfamethoxazole [25], acid orange 7 [26,27], methyl orange [25,26], bisphenol A [25], and methylene blue [25,28]. The activation process of peroxymonosulphate includes the used of different catalysts, such as perovskites [23], atom-dispersed Co in a boron-carbon-nitrogen matrix [24], functionalized Co_3O_4-Bi_2O_3-Ti membranes [25], copper ferrite nanoparticles [26], graphitic carbon nitride/ε-manganese dioxide microspheres [27], and nitrogen-doped porous carbon [28]. Advances in different strategies for the degradation of organic pollutants have been extensively explored due to the harmful effects of these compounds on the water environment and public health [24,26]. Moreover, interactions of emerging contaminants with microorganisms in both bulk water and biofilms have been reported [29-31]. Additionally, persulphates are relatively less expensive compared to other oxidizing agents used in advanced oxidation processes [32-34]. On the other hand, a comparable fewer number of studies have reported the disinfection of suspended microorganisms by OXONE, including the inactivation of *Escherichia coli*, *P. aeruginosa*, spores of *Bacillus atrophaeus* and *Bacillus thuringiensis*, as well as fungal spores of *Cladosporium cladosporioides*, *Penicillium polonicum*, *Aspergillus niger*, and *Trichoderma harzianum* [35-38]. The destabilization of the cell membrane was proposed as its principal mode of antimicrobial action [38,39]. Recently, OXONE was indicated as a promising alternative to free chlorine for the control of biofilms developed by DW-isolated bacteria [39]. The exposure of 48 h-old biofilms of *Acinetobacter calcoaceticus* and *Stenotrophomonas maltophilia* to OXONE for 30 min caused up to 5 log reduction of biofilm culturable cells, with superior efficacy than free chlorine [39]. Nevertheless, the previous study limited the evaluation of the effects on biofilm control by the use of microtiter plates. These platforms allow high-throughput screening of the effects of different disinfectants against biofilms. However, microtiter plates provide operating conditions for biofilm formation far from mimicking those encountered in DWDS [40].

The present work aimed to validate the potential of OXONE to control DW biofilms in comparison to chlorine disinfection under realism-based conditions. The effects of disinfectants were evaluated against 7 day-old *S. maltophilia* biofilms formed under conditions mimicking DWDS. DW-isolated *S. maltophilia* was used as a model bacterium for biofilm formation because it is recognized as an emerging and opportunistic multidrug-resistant pathogen [41-45]. For instance, an outbreak of *S. maltophilia* in an intensive care unit was reported to be associated with the presence of biofilms in devices for DW supply [46]. In this study, a rotating cylinder reactor (RCR) was used for the simulation of a DWDS and has been already validated for the formation of DW biofilms [16,47]. The chemical stability of OXONE and chlorine solutions in STW at 25 ºC was evaluated over 40 days. Moreover, the reactive species produced during the OXONE disinfection in STW were identified by electron paramagnetic resonance analysis.

2. Materials and methods

2.1. Chemicals

Pentapotassium bis(peroxymonosulphate) bis(sulphate) (OXONE), which was selected from the product type 5 Article 95 List of the Biocidal Products Regulation published by ECHA [48], and 2,2′-azino-bis(3-ethylbenzothiazoline-6-sulfonic acid) diammonium salt (ABTS) were purchased from Sigma-Aldrich (St. Louis MO, USA). Calcium hypochlorite (Merck, Darmstadt, Germany) was used as reference disinfection by free chlorine release [11]. Free chlorine concentration was determined through the DPD (N,N-diethyl-p-phenylenediamine) colorimetric method using the HI96701 free chlorine portable photometer (Hanna Instruments) [39,49]. Stock solutions of OXONE and free chlorine were freshly prepared in ultrapure water or sterile STW, which was composed of 100 mg/L $NaHCO_3$ (Merck, Darmstadt, Germany), 13.4 mg/L $MgSO_4 \cdot 7\ H_2O$ (Labkem, Barcelona, Spain), 0.7 mg/L K_2HPO_4 (VWR BDH CHEMICALS, Leuven, Belgium), 0.3 mg/L KH_2PO_4 (VWR BDH CHEMICALS, Leuven, Belgium), 0.01 mg/L $(NH_4)_2SO_4$ (Panreac, Barcelona, Spain), 0.01 mg/L NaCl (Merck, Darmstadt, Germany), 0.001 mg/L $FeSO_4 \cdot 7\ H_2O$ (VWR BDH PROLABO, Leuven, Belgium), 1 mg/L $NaNO_3$ (VWR BDH CHEMICALS, Leuven, Belgium), 27 mg/L $CaSO_4$ (Labkem, Barcelona, Spain), and 1 mg/L humic acids (Sigma-Aldrich, Sintra, Portugal) [50], and stored at 4 ºC. DMPO (5,

5-dimethyl-1-pyrroline-*N*-oxide) was purchased from TCI Chemicals (Portland, OR, USA). 4-oxo-TEMP (2,2,6,6-tetramethyl-4-piperidone hydrochloride) was purchased from Sigma-Aldrich (Darmstadt, Germany).

2.2. Biofilm formation

Mature biofilms were formed according to Gomes et al. [16] with some modifications, using an RCR under mimicking conditions in DWDS. A detailed description of the structure and functioning of the RCR can be found elsewhere [16,51]. *S. maltophilia* isolated from DW [52] was used in this study. Two 1 L Erlenmeyer flasks containing 250 mL of R2A broth were inoculated with *S. maltophilia* colonies and incubated overnight at 25 ± 2 ºC and 120 rpm. Cells were harvested by centrifugation at 3220 × *g* for 10 min, washed, and resuspended in 500 mL of R2A broth. The reactor was then inoculated with the bacterial suspension and diluted with STW to a final volume of 5 L and a final cellular density of approximately 2.5×10^7 CFU/mL. Polyvinyl chloride (PVC) cylinders were used for biofilm formation with a sampling area of 39.27 cm^2 ($d = 2.5$ cm; $l = 5$ cm) per cylinder. This material was chosen as a representative pipe material from DW networks [47,53,52]. The cylinders rotated under constant speed equivalent to a liquid flow of 0.1 m/s and shear stress on the cylinder surface of 0.1 Pa, similar to typical conditions found in plumbing systems [54,16,55,56]. The RCR operated under batch conditions for 7 h to promote initial bacterial adhesion. Afterwards, silicone tubing and a peristaltic pump operating at 0.5 L/h were used to continuously feed the reactor with 10 × diluted R2A broth from a polypropylene 50 L feed carboy, ensuring a hydraulic retention time (HRT) of 10 h [16,47]. To obtain mature and steady-state biofilms, the RCR operated for 7 days [16,51,57]. STW and 10 × diluted R2A broth were selected as culture media for biofilm formation instead of real tap water, to optimize the required run time for the experiments and prevent reproducibility issues inherent to the natural changes of the characteristic of DW supplied by municipal water networks [16,47].

2.3. Biofilm characterization

At the end of the operation time, each cylinder was removed from the RCR and carefully washed in STW to remove non-adhered bacteria. Then, biofilms formed in the RCR were characterized in terms of wet mass, culturable cells, total and intact membrane bacteria, and content of extracellular proteins and polysaccharides. The wet mass was obtained by the difference between the mass of the cylinder with biofilm and the mass of the cylinder without biofilm. The biofilms were removed from the cylinder surfaces by scrapping four times for 1 min using 5 mL pipette tips and rinsing each time with 2.5 mL of extraction buffer (0.76 g/L $Na_3PO_4 \cdot 12\ H_2O$ (Merck, Darmstadt, Germany), 0.4 g/L $Na_2HPO_4 \cdot 2\ H_2O$ (Chem-lab, Belgium), 0.53 g/L NaCl and 0.08 g/L KCl at pH 7), resuspending the biofilms in a total of 10 mL of extraction buffer. The suspensions were further vigorously vortexed for 2 min to homogenize. Culturable bacteria were determined after 48 h of incubation at 25 ± 2 ºC on R2A agar. The results are presented as log CFU/cm^2. Total cells and those with no damaged membrane were determined by epifluorescence microscopy using the Live/Dead BacLight™ bacterial viability kit (Invitrogen, Waltham MA, USA), where SYTO9 labels all bacteria while propidium iodide labels only membrane damaged bacteria. Bacteria with intact membranes (green stained cells) and the total number of cells (sum of green and red stained cells) were assessed by cell counting of a minimum of 15 fields of view. The results are presented as log cells/cm^2 and the detection limit of the method is 4.8 log cells/cm^2 [16]. For the analysis of extracellular proteins and polysaccharides content, a procedure for extraction and quantification of EPS was performed according to Frølund et al. [58] and Gomes et al. [16]. The extraction occurred under 400 rpm at 4 ºC for 4 h with Dowex® Marathon© resin, followed by centrifugation at 3220 × *g* for 5 min for separation of EPS from the bacterial cells. Peterson's modification of the micro Lowry method [59,60] was used for the quantification of proteins, using bovine serum albumin as standard. The polysaccharides were quantified according to the phenol-sulfuric method [61], using glucose as the standard.

2.4. Biofilm exposure to disinfectants

Solutions of OXONE and free chlorine in STW were prepared at 10 × minimum bactericidal concentration (MBC) of each disinfectant against *S. maltophilia*. The MBC values of 340 mg/L for OXONE (*i.e.,* 553 μM) and 0.8 mg/L for free chlorine (*i.e.,* 22.6 μM) were determined in a previous study [39] and considered to be the lowest concentrations under which complete growth absence in planktonic cultures was detected. Cylinders with biofilms were carefully washed in STW to remove non-adhered bacteria. Then, biofilms were exposed to 200 mL of OXONE or free chlorine solutions for 30 min in a 250 mL glass beaker. At the end of the exposure time, the cylinders were carefully immersed in STW to wash the disinfectants, followed by a similar procedure as described above, which included scrapping and resuspending the biofilms in 10 mL of neutralizer solution, which its detailed composition can be found elsewhere [39,62]. The samples were analysed in terms of culturability, the presence of cells with non-damaged membranes and total cells, as described previously. Unexposed biofilms (control samples) were performed by replacing the disinfectant solution for STW.

2.5. Chemical stability of OXONE and free chlorine solutions

The stability of OXONE and free chlorine solutions were evaluated as the depletion of each disinfectant at 25 ± 2 ºC for 40 days. The solutions were prepared in STW and ultrapure water at 10 × MBC of each disinfectant against *S. maltophilia* and stored in light-protected flasks. The concentration of OXONE was determined by spectrophotometric measurement using ABTS as an indicator and according to the method described by Zou et al. [63]. A stock solution of ABTS was prepared at 50 mM in ultrapure water and stored at 4 ºC. Phosphate buffer solution at 50 mM and pH 7 was prepared by mixing 38.5 mL of KH_2PO_4 (VWR BDH CHEMICALS, Leuven, Belgium) stock solution (0.5 M) with 61.5 mL of $K_2HPO_4 \cdot 3\ H_2O$ (Fisher Scientific, Leicestershire, UK) stock solution (0.5 M) and diluting the combined stock solutions to 1 L with ultrapure water. The OXONE standards solutions were freshly prepared in ultrapure water in the range of 50–1000 mg/L. For measuring OXONE concentration, the procedure was as follows: 2.25 mL of phosphate buffer solution and 0.125 mL of ABTS solution were firstly added into appropriately labelled test tubes; then 0.125 mL of OXONE standard solutions or water samples containing OXONE were orderly added into the test tubes; the mixed solutions were left to react for 10 min at room temperature (23 ± 2 ºC) in the dark; and finally, the absorption value of the mixed solutions at 415 nm was recorded using a spectrophotometer (V-1200 Spectrophotometer VWR, Leuven, Belgium). The mixed solution without OXONE (*i.e.*, replacing it with 0.125 mL of ultrapure water) was used as the blank solution. When necessary, the water samples containing OXONE were appropriately diluted in ultrapure water before the reaction. The over time depletion of free chlorine was evaluated according to the DPD colorimetric method. When possible, a linear regression was performed to the experimental data to quantify the disinfectant depletion. The slope of the linear model corresponded to the disinfectant loss rate $\left(\frac{dC}{dt}\right)$ (mg/L/day) and the Y-intercept represented the estimated initial value of disinfectants (mg/L). Additionally, the half-life $t_{1/2}$ (days) for the free chlorine to be reduced by 50% was calculated from the linear models. The goodness of fit was evaluated based on the coefficient of determination (R^2).

2.6. Electron paramagnetic resonance studies

To identify the reactive oxygen species (ROS) formed during the

disinfection of *S. maltophilia* by OXONE at MBC in STW, EPR studies were performed in the conditions of the process. EPR spectra were recorded using a Bruker ELEXSYS E500 spectrometer, available at Laboratory for Electron Paramagnetic Resonance Spectrometry (CEMUP – Centro de Materiais da Universidade do Porto), operating at 9 GHz (X-band) using the following general experimental conditions, as specified below for each type of radical detection. Xepr software (Bruker) was used for spectra acquisition and Easyspin-5.2.35 for computer simulations and calculation of the Spin Hamiltonian parameters. The relative amount of radical formed was estimated by integration of the EPR signal (area under the curve, AUC) using Origin 2015 software [64]. All experiments were carried out under room light (only artificial light at constant intensity was present) and samples were protected from the light with aluminium foil.

For the investigations regarding the production of singlet oxygen radical ($^1O_2$), a stock solution of 4-oxo-TEMP spin trap was freshly prepared before analysis at 14 mg/mL in distilled water. Then, 70 μL of 4-oxo-TEMP solution was added to 1 mL of bacterial test mixture. The bacterial test mixture containing a final cellular density of approximately 10^7 CFU/mL had been prepared in OXONE solution instants before the addition of the spin trap by mixing 100 μL of bacterial solution in PBS, 100 μL of STW at 10 × its final concentration, and 800 μL of OXONE solution in ultrapure water at 1.25 × the required test concentration [39,62]. An aliquot was quickly collected and placed in a capillary tube, which was then placed in the quartz EPR tube for spectra acquisition. Spectra were recorded at defined time points (0, 10, 20, and 30 min of disinfection) and the following general experimental conditions: room temperature (20 ± 2 ºC), the modulation frequency of 100 kHz, microwave power 6 mW, modulation amplitude 4 Gauss (G), 60 dB of receiver gain, the acquisition time of 50 s and 5 scans.

To study the production of superoxide ($O_2^{\bullet-}$), hydroxyl ($HO^{\bullet}$), and sulphate ($SO_4^{\bullet-}$) radicals, a stock solution of DMPO spin trap was freshly prepared before analysis at 18 mg/mL in distilled water. Then, 70 μL of DMPO solution was added into 1 mL of bacterial test mixture as described above. An aliquot was quickly collected and placed in a capillary tube, which was then placed in the quartz EPR tube for spectra acquisition. Spectra were recorded at defined time points (0, 10, 20, and 30 min of disinfection) and the following general experimental conditions: room temperature (20 ± 2 ºC), the modulation frequency of 100 kHz, microwave power 4 mW, modulation amplitude 4 G, 60 dB of receiver gain, the acquisition time of 220 s and 5 scans.

2.7. Statistical analysis

A minimum of three independent assays were performed in duplicate for each condition tested. Results are presented as mean and standard deviation (SD). The ordinary one-way ANOVA test followed by Tukey's multiple comparisons test was performed for the statistical analysis. A confidence level ≥ 95% ($P < 0.05$) was considered in the statistical analysis, using GraphPad Prism 9 for Windows.

3. Results and discussion

3.1. Effects of OXONE on mature biofilms

The RCR was used for biofilm formation under conditions mimicking DWDS. *S. maltophilia* biofilms were formed for 7 days on PVC cylinders under constant rotation speed similar to the typical water velocity in plumbing systems (0.1 m/s) [54,16,55,56]. Before exposure to disinfectants, biofilms were characterized in terms of wet mass, culturability, total and non-damaged bacteria, and content of extracellular proteins and polysaccharides (Table 1). The numbers of culturable and total cells were in the same magnitude, respectively, 7.6 ± 0.5 log CFU/cm^2 and 7.4 ± 0.4 log cells/cm^2. Usually, the level of biofilm cell density is one order of magnitude higher than the number of biofilm culturable cells, however, the results were between the range of CFU and cell densities of biofilms reported within DWDS [65-67]. The number of non-damaged cells represented 97% of the total biofilm cell density. Regarding the content of EPS, the level of extracellular proteins (519 ± 146 μg/g $_{biofilm}$) was approximately equal to the level of extracellular polysaccharides (460 ± 91 μg/g $_{biofilm}$). Conversely, Gomes et al. [16,50] reported contents of extracellular polysaccharides of *S. maltophilia* biofilms formed in the RCR higher than the levels of extracellular proteins. The different EPS composition of the biofilms could be related to the use of distinct surface materials [16,53,68] or different broth media compositions for biofilm formation [47].

Table 1
Characterization of biofilms formed in the rotating cylinder reactor.

	S. maltophilia biofilms on PVC cylinders
Wet mass, mg/cm^2	4.1 ± 1.2
Culturable cells, log CFU/cm^2	7.6 ± 0.5
Total cells, log cells/cm^2	7.4 ± 0.4
Biofilm viability, log non-damaged cells/cm^2	7.2 ± 0.5
Extracellular proteins, μg/g $_{biofilm}$	519 ± 146
Extracellular polysaccharides, μg/g $_{biofilm}$	460 ± 91

The characteristics of DW biofilms are very dependent on the conditions found in real DWDS, namely the type of pipe materials, the age of the pipelines, the layout of the network, hydrodynamic conditions, and the composition of the water, among others [3,4]. The challenging task of studying biofilms in real DWDS encourages the use of biofilm reactors, which strive to ensure that the operating conditions (*i.e.,* physical, chemical and biological parameters) are as similar as possible to those found in real scenarios [40]. Previous studies demonstrated the suitability of the RCR to study biofilms under conditions simulating DWDS [16,47]. Nevertheless, the comparison of the characteristics of biofilms in model systems with those formed in real DWDS is an arduous assignment given the limited number of studies with the evaluation of the exact same biofilm properties and methods of quantification. Most of these studies with biofilm samples of real DWDS focused only on the determination of the total and culturable cell densities or microbial community evaluation under different operational conditions [66,69]. In this study, the biofilms developed using the RCR presented total and culturable cells numbers comparable to those reported using other biofilm reactors fed with tap water for two to four months (heterotrophic plate counts approximately 10^7 to 10^8 CFU/cm^2 and a total number of biofilm cells approximately 2 × 10^7 cells/cm^2) [66,69]. Additionally, Shen et al. [70] reported a ratio of protein to polysaccharide close to 1 for biofilms formed in CDC reactors with PVC coupons and fed by groundwater for three months.

Then, biofilms were exposed to OXONE and free chlorine at 10 × MBC in STW for 30 min and the effects were evaluated in terms of biofilm culturability, biofilm cell density and number of non-damaged cells (Fig. 1). The exposure of the 7 day-old biofilms to disinfectants promoted a statistically significant ($P < 0.05$) reduction of biofilm culturability in comparison to the unexposed/control biofilms of approximately 1 log reduction with free chlorine and 4 log reduction with OXONE. Remarkably, the action of OXONE in decreasing biofilm culturable cells was more efficient than the exposure of biofilms to free chlorine ($P < 0.05$). Considering the biofilm cellular density, no significant differences ($P > 0.05$) were observed in the total number of cells in biofilms after exposure to the disinfectants. Unexposed biofilms (control group) or those exposed to the disinfectants presented total levels of cells approximately of 7 log cells/cm^2. However, the exposure of the 7 day-old *S. maltophilia* biofilms to free chlorine and OXONE promoted a significant decrease ($P < 0.05$) in the number of non-damaged cells. Notably, biofilms exposed to OXONE presented levels of non-damaged cells below the detection limit of 4.8 log cells/cm^2, whereas the exposure to free chlorine only allowed a decrease of non-damaged cells to 6.4 ± 0.5 log cells/cm^2 ($P < 0.05$) (Fig. 1).

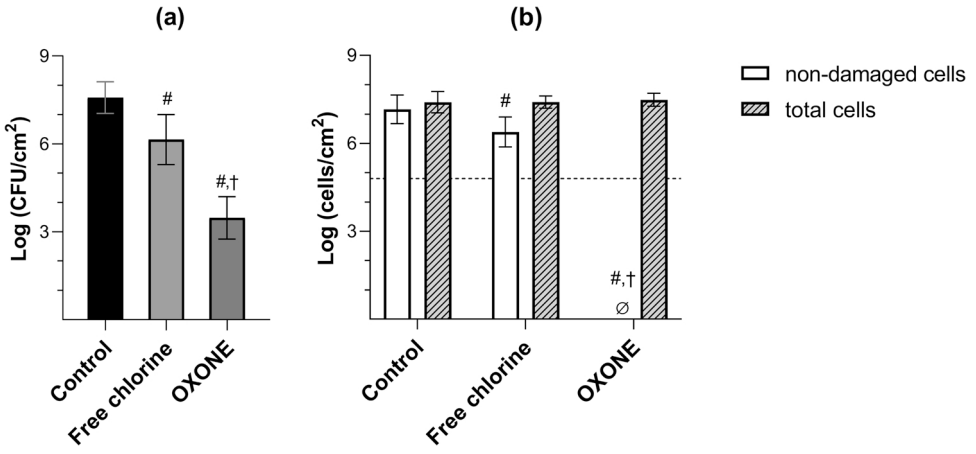

Fig. 1. The effects of free chlorine and OXONE at 10 × MBC in STW against 7 day-old *S. maltophilia* biofilms formed in the RCR. **(a)** biofilm culturable cells. **(b)** biofilm cellular density: number of non-damaged cells (solid-white bars) and total cells (patterned bars). ø below the detection limit of 4.8 log cells/cm^2 (dashed line). # indicates statistically significant differences to control/unexposed biofilms. † indicates statistically significant differences to biofilms exposed to free chlorine.

The results demonstrated that the treatment with OXONE was efficient to control mature *S. maltophilia* biofilms formed under conditions mimicking DWDS. The biofilms exposed to OXONE were substantially inactivated, resulting in more than a 4 log reduction in biofilm culturability and the number of non-damaged cells. However, it was unable to remove the biofilms from the PVC surface since the number of total cells in the biofilms was not decreased by OXONE in comparison to the control (Fig. 1b), which is also in accordance with Oliveira et al. [39]. Moreover, the action of OXONE was significantly better than the exposure to free chlorine, which only allowed a reduction in biofilm culturability and the number of non-damaged cells in the order of 1 log. The inability of chlorine to control biofilms was already reported by other authors [71,16,72]. Gomes et al. [16] demonstrated that free chlorine at 10 mg/L for 10 min did not reduce the number of non-damaged membrane and culturable cells of 7 day-old *S. maltophilia* biofilms grown on stainless steel, copper, and 57% copper alloy. High levels of chlorination (between 50 and 200 mg/L for 2 h) decreased the number of culturable cells in 18 and 30 day-old *L. pneumophila* biofilms on galvanized steel and PVC, however, biofilms were not eradicated and continued to grow on subsequent days [71]. Moreover, detached cells from 90 day-old *E. coli* biofilms formed on plastic-based materials (PVC, polypropylene, and polyethylene) were eradicated by chlorine, but *E. coli* cells from biofilms formed on iron pipes could resist the chlorine treatment [72]. Furthermore, it should be pointed out that the exposure of biofilms to OXONE in STW, which has chloride ions (Cl^-) in its composition, could overestimate the effects of OXONE because the production of hypochlorous acid (HOCl) was reported to be generated from saltwater oxidation of peroxymonosulphate [37,73]. Nevertheless, the present results are in agreement with the effects of OXONE at the same concentration in ultrapure water against established 48 h-old *S. maltophilia* biofilms, where an approximately 4 log reduction was also observed (unpublished results).

3.2. Evaluation of the chemical stability of OXONE and free chlorine solutions

Among different factors, the control of microbial proliferation in DWDS is mainly dependent on the maintenance of residual disinfectant concentration through the water distribution network [3,4]. Maintaining an effective free chlorine residual concentration is known to be a challenge given the existence of chemical reactions occurring both in the bulk phase and at the pipe walls that contribute to chlorine decay in DWDS [74-77]. Therefore, the chemical stability of OXONE solutions in ultrapure water and STW was evaluated as disinfectant depletion over time and compared to the free chlorine decay in the same conditions. The initial disinfectant concentrations were prepared at the correspondent 10 × MBC of each disinfectant against *S. maltophilia* and the temperature was controlled at 25 ºC for 40 days.

The analysis of Fig. 2a demonstrated that after an initial drop of OXONE concentrations during the first 9 days of the experiment, the OXONE solutions were mainly stable over time, both in ultrapure water and in STW. The median values of OXONE concentrations in ultrapure water and in STW were approximately 2700 mg/L and 2500 mg/L, respectively. The interquartile range of OXONE concentrations in ultrapure water was 2600–2800 mg/L. In STW, the interquartile range was 2400–2600 mg/L. A linear regression was performed on the experimental data to quantify the OXONE depletion during the first 9 days (Fig. 2b). The results of the OXONE loss rate and statistical measures of the linear models are presented in Table 2. The OXONE loss rate $\left(\frac{dC}{dt}\right)$ in STW and ultrapure water was -70.4 ± 13.4 and -66.1 ± 9.0 mg/L/day, respectively. No statistical difference ($P > 0.05$) was observed between the linear regression of OXONE depletion in STW and in ultrapure water. Therefore, the overall results indicate that the presence of inorganic and organic substances in STW had a small or inexistent impact on OXONE depletion over the 40 days of the experiment, resulting in OXONE concentrations approximately equal to the values obtained in the solution without interfering agents. However, in both conditions, the OXONE solutions presented a disinfectant depletion of approximately 10% of the initial OXONE concentrations within the first 9 days, after this time the values of OXONE concentration became stagnated. Considering that the initial OXONE depletion of 10% was observed both in STW and ultrapure water (*i.e.*, no interfering substances), the results suggest that this decrease in OXONE concentration may be attributed to the peroxide bond activation by thermolysis [22]. Indeed, the incubation of disinfectant solutions was performed at 25 ºC, the threshold temperature value which water utilities in some countries are asked to comply with, and the maximum water temperature limit at the tap recommended by the WHO guidelines [11,78].

To evaluate the chemical stability of free chlorine, its concentration over time in ultrapure water and STW was measured and is presented in Fig. 3. The linear regression of the experimental data allowed the assessment of the kinetic parameters that quantify chlorine decay (Table 3). The absolute value of the chlorine loss rate $\left(\frac{dC}{dt}\right)$ in STW, 0.078 ± 0.005 mg/L/day, was significantly ($P < 0.05$) higher than the loss rate $\left(\frac{dC}{dt}\right)$ in ultrapure water, 0.022 ± 0.002 mg/L/day. Moreover, the half-life ($t_{1/2}$) calculated for chlorine depletion in STW was approximately 45 days, whereas in ultrapure water the $t_{1/2}$ was approximately 198 days ($P < 0.05$). Over the 40 days of the experiment, the free

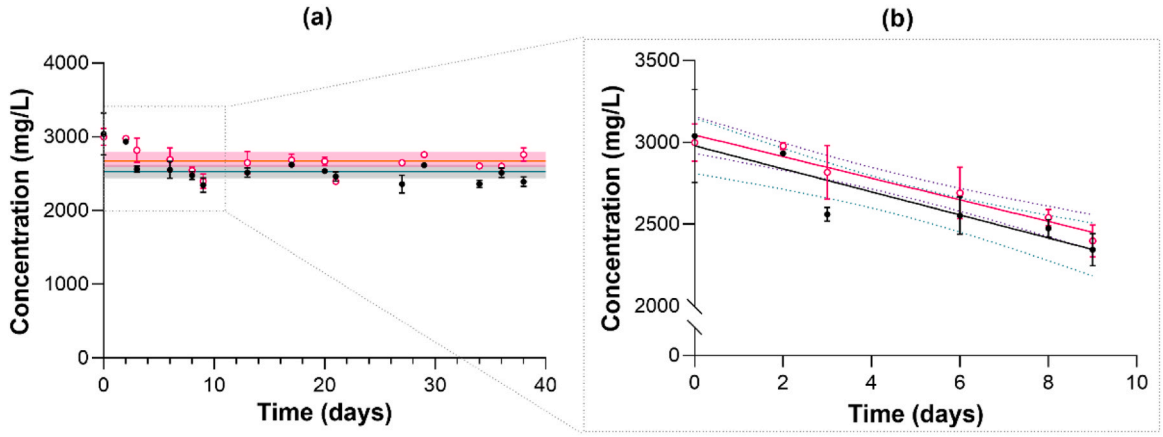

Fig. 2. Time course of chemical stability of OXONE in ultrapure water (open magenta circles) and STW (closed black circles) solutions at 25 ºC in light-protected conditions. (a) over the 40 days of the experiment. The blue and orange lines represent the median of OXONE concentrations in STW and in ultrapure water, respectively. Shade zones define the interquartile range of OXONE concentrations in STW and ultrapure water. (b) zoom in on OXONE concentration in the first 9 days of the experiment. Solid lines represent the linear regression of the experimental data. Dashed lines define the 95% confidence band of the model.

Table 2
Kinetic parameters and statistical measures of the linear regression of the experimental data from the chemical stability evaluation for OXONE over the first 9 days of the experiment.

Parameters	Ultrapure water	STW
Slope $= \frac{dC}{dt}$, mg/L/day	-66.1 ± 9.0	-70.4 ± 13.4
Y-intercept, mg/L	3046 ± 51	2980 ± 76
R^2	0.8444	0.7347

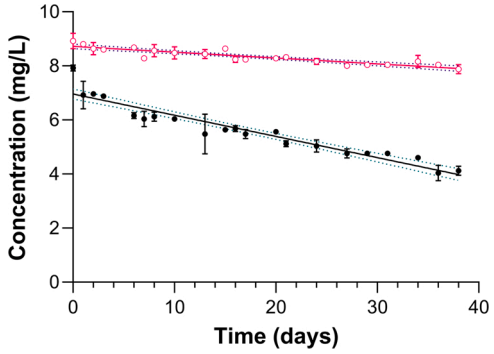

Fig. 3. Concentration of free chlorine (mg/L) over 40 days in ultrapure water (open magenta circles) and STW (closed black circles) solutions at 25 ºC in light-protected conditions. Solid lines represent the linear regression of the experimental data. Dashed lines define the 95% confidence band of the model.

Table 3
Kinetic parameters and statistical measures of the linear regression of the experimental data of free chlorine depletion in ultrapure water and STW, over the 40 days of the experiment.

Parameters	Ultrapure water	STW
Slope $= \frac{dC}{dt}$, mg/L/day	-0.022 ± 0.002	-0.078 ± 0.005
Y-intercept, mg/L	8.72 ± 0.04	7.00 ± 0.09
R^2	0.7331	0.8834
$t_{1/2}$, days	198	45

chlorine depletion in STW was approximately 48% of the initial value, revealing a possible reaction of chlorine with the inorganic and organic substances of STW [74]. Indeed, the reactions of chlorine with inorganic substances in natural waters are relatively quick and, generally, involve compounds such as ammonia, halides, iron, and sulphide [74,79]. Whereas low chlorine reaction rates with organic compounds are commonly observed during chlorination [74,79]. In the present work, chlorine in ultrapure water was mainly stable, with approximately 11% of free chlorine depletion over the 40 days of the experiment. In fact, without interference substances, sodium hypochlorite at 25 ºC demonstrated to be more stable than neutral electrolysed oxidizing water, chlorine dioxide, and sodium dichloroisocyanurate solutions [49].

Although the promising activity and stability of OXONE, the economic perspective from its use is potentially limiting. In general, persulphates are recognized as relatively less expensive than other oxidants used in advanced oxidation processes [33,34]. However, chlorine seems to have lower costs. The OXONE salt ($2KHSO_5 \cdot KHSO_4 \cdot K_2SO_4$) was evaluated by 2.2 USD/kg [34]. On the other hand, the price of chlorine in the USA market by July 2023 was evaluated by 0.91 USD/kg [80], and DW treatment plants with a daily flow rate of 100 m^3 can present an average cost of CAN$1.00 to produce DW by chlorination [81]. However, the economic advantage of chlorine can dissipate with the increase in the volume of treated water, due to economies of scale, as observed when compared to other DW disinfection methods [82]. Furthermore, if in real DWDS the use of OXONE could lead to a lower likelihood of occurrence of microbiological problems, as demonstrated in the present work, the choice of the disinfectant cannot be based exclusively on cost comparisons.

3.3. *Identification of reactive species produced during disinfection with OXONE*

Research on advanced oxidation processes for oxidative degradation of organic pollutants indicates that persulphates have a strong oxidizing action via two-electron reduction, and decomposition into sulphate and hydroxyl radicals by cleaving the peroxide bond [22,83,34]. However, the mechanism behind the disinfectant activity of OXONE has not been fully elucidated and is limited to a few studies [35,37,39]. Therefore, in the present work, the activity of OXONE against *S. maltophilia* was monitored by EPR spectroscopy, to get insight into its mechanism of disinfection. The experiments were performed considering STW to simulate microbial disinfection for application in the treatment of DW.

Studies using spin trap 4-oxo-TEMP were performed aiming to detect singlet oxygen radicals ($^1O_2$) eventually formed during the disinfection of *S. maltophilia* with OXONE. This spin trap forms an adduct with $^1O_2$, which can be detected by EPR [84]. The spectra obtained are depicted in Fig. 4a and Fig. 4b and exhibit the typical (1:1:1) triplet signal and *g*

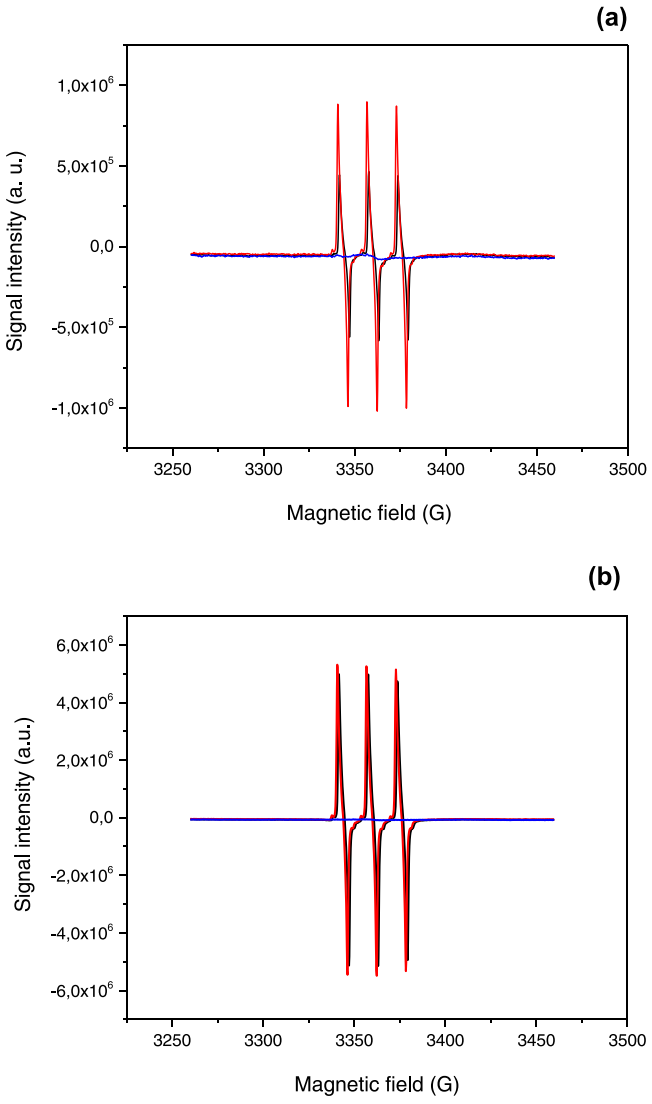

Fig. 4. Representative EPR spectra of singlet oxygen radical production at time zero (a) and after 30 min (b) of *S. maltophilia* exposure to OXONE in STW. A. u. means arbitrary units. The blue line represents the blank sample (bacterial cells in STW without exposure to OXONE); the black line represents the control sample (OXONE in STW without bacterial cells); the red line represents the test sample (bacterial cells exposed to OXONE in STW).

value (g = 2.0067) of the adduct 4-oxo-TEMP-singlet oxygen radical [84-87]. The relative amount of trapped $^1O_2$ over 30 min is presented in Fig. 5a.

The formation of $^1O_2$ radicals was immediately confirmed at time zero with high-intensity EPR signals registered for OXONE solutions in STW, with and without the presence of bacterial cells (Fig. 4a). Over the 30 min of analysis, the intensity of the signals significantly increased, in both conditions (Fig. 4b and Fig. 5a). However, no statistically significant differences ($P > 0.05$) were observed in the relative amount of $^1O_2$ trapped in the presence or absence of *S. maltophilia* cells. The results suggested that OXONE is activated by the presence of inorganic and organic substances in STW, allowing the generation of $^1O_2$ radicals. During the disinfection process of *S. maltophilia* by OXONE in STW, the presence of $^1O_2$ radicals was also detected, but there was no evidence of an increase in $^1O_2$ generation from the inactivation of *S. maltophilia*.

A study on base-catalysed hydrolysis of OXONE to sulphate anion and hydrogen peroxide proved that $^1O_2$ and superoxide ($O_2^{\bullet-}$) radicals were the primary reactive oxygen species in the system, resulting in the degradation of a variety of organic pollutants [86]. The possible activation mechanism was supported by the radical quenching method (*tert*–butyl alcohol, methanol, sodium azide, and *p* –benzoquinone) and electron spin resonance trapping studies [86]. The present work also confirmed the presence of $^1O_2$ radicals during microbial exposure to OXONE that may be involved in the mechanism of *S. maltophilia* inactivation. Indeed, $^1O_2$ radicals are known to oxidize many biological molecules, such as proteins, nucleic acids, and lipids, resulting in cell damage [88-91].

Superoxide ($O_2^{\bullet-}$), hydroxyl ($HO^{\bullet}$), and sulphate ($SO_4^{\bullet-}$) radicals have been reported to participate in the antimicrobial mechanism of action of activated persulphates, mainly peroxydisulphate [37,92-94]. Therefore, the DMPO spin trap was used to detect the formation of these radicals in the disinfection process by OXONE in STW. The spectra obtained are depicted in Fig. 6 and the relative amount of radicals trapped over 30 min is presented in Fig. 5b. A weak EPR signal was detected, and its intensity strengthened over time. After 20 and 30 min of *S. maltophilia* exposure to OXONE in STW, the relative quantity of trapped radicals was statistically significantly higher ($P < 0.05$) than in the OXONE solution in STW without bacterial cells. However, despite our efforts, it was not possible to assign the detected EPR signal to specific radical species formed in the process. The obtained signal did not correspond to the typical shapes of DMPO-OH, DMPO-SO_4, and DMPO-OOH adducts [86,95,94], so it must correspond to another non-identified free radical. Qi et al. [86] and Wei et al. [95] reported a signal presenting four characteristic lines which were attributed to a DMPO-OH adduct (1:2:2:1) with hyperfine coupling constants of a_N between 14.9 and 15.0 G and a_H between 14.7 and 14.9 G. Also, spectra showing six characteristic lines were assigned as a DMPO-OOH adduct with $a_N \approx 14$ G and $a_H \approx 8$ G and a DMPO-SO_4 adduct (1:1:1:1:1:1) with $a_N \approx 14$ G, $a_{\beta\text{-H}} \approx 10$ G, $a_{\gamma\text{-H1}} \approx 1.5$ G, and $a_{\gamma\text{-H2}} \approx 0.8$ G [86,95,94].

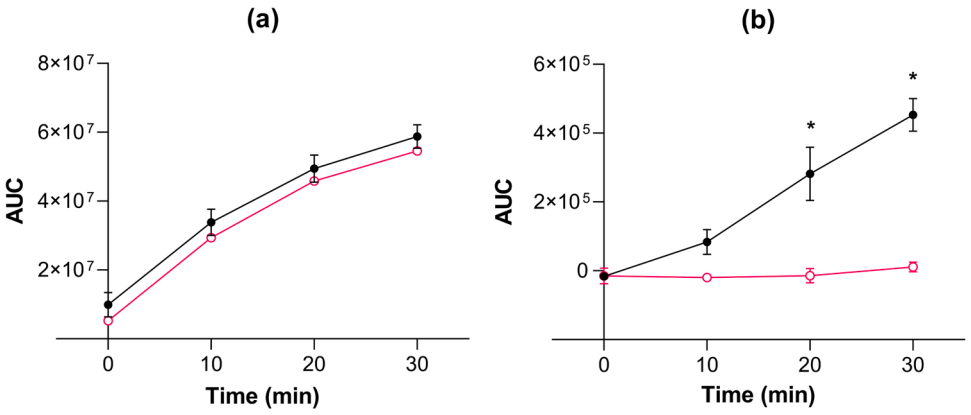

Fig. 5. Time course of reactive species generation during the disinfection of *S. maltophilia* by OXONE in STW. (a) 4-oxo-TEMP spin trapped singlet oxygen radicals. (b) DMPO spin trap detected other radicals. Closed black circles represent test samples (bacterial cells exposed to OXONE in STW). Open magenta circles represent control samples (OXONE in STW without bacterial cells). The values represent the area under the curve (AUC) of the EPR spectra for each condition subtracted by AUC of the blank samples (bacterial cells in STW without exposure to OXONE). * indicates statistically significant differences to the control sample ($P < 0.05$).

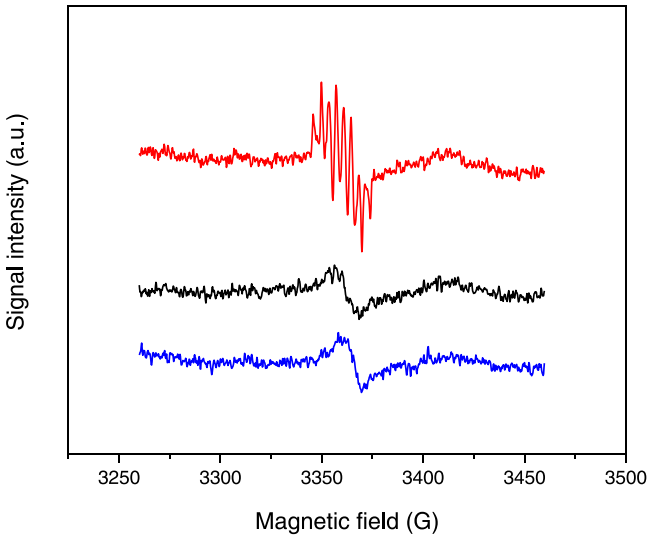

Fig. 6. Representative EPR spectra of radicals trapped by DMPO after 30 min of *S. maltophilia* exposure to OXONE in STW. The blue line represents the blank sample (bacterial cells in STW without exposure to OXONE); the black line represents the control sample (OXONE in STW without bacterial cells); the red line represents the test sample (bacterial cells exposed to OXONE in STW).

Nevertheless, the shape of the EPR spectrum of the free radical detected in the present work does not match any of the commonly reported ones for the radicals adducts formed with the DMPO spin trap.

Regarding the study of the presence and contribution of the specific reactive species on microbial inactivation by persulphates, to the best of the authors' knowledge, there is only one published study that has examined the disinfection mechanism through EPR analysis. Xia et al. [94] reported that the dominant reactive species responsible for the *E. coli* K-12 inactivation with peroxydisulphate activated by magnetic pyrrhotite were sulphate and hydroxyl radicals. In that work, the evaluation of the mechanism of inactivation was based on the integration of EPR analysis and a positive scavenging test using methanol for $SO_4^{\bullet}$, *tert*-butyl alcohol for $HO^{\bullet}$, Fe(II)-EDTA for H_2O_2, and TEMPOL for $O_2^{\bullet-}$ [94]. Other studies evaluated the major contributing radicals in microbial inactivation only by indirect methods, such as through the quantification of the degradation of chemical probes, pathogen survival with the presence of radical scavengers, and theoretical models [37,92,96,93]. The specific reactive species responsible for the antimicrobial activity appear to be dependent on the method of persulphate activation, for instance, Cu(II) or Fe(II) catalysis, ultraviolet (UV) photolysis, or alkali activation [37,92,96,93]. Particularly, in the Cu(II)-activated peroxymonosulphate system, $SO_4^{\bullet-}$ was the dominant reactive oxidant present in the inactivation of *P. aeruginosa* [37]. Additionally, *P. aeruginosa* demonstrated to promote the production of reactive oxidants, given the increase in the degradation of a chemical probe (phenol) with an increasing population of bacterial cells [37]. However, one should be cautious when interpreting findings of the mechanism of action based on indirect methods, as highlighted in a recent work that proved the invalidity of quenching methods for the persulphate-based processes [97]. The misinterpretation of the role of the reactive species in these systems can be caused by an increase of peroxymonosulphate decomposition, interfering reactive species generation, and scavenging of non-target reactive species in the presence of high-concentration quenchers [97].

4. Conclusions

The purpose of the current study was to validate the capability of OXONE to control DW biofilms formed under realism-based conditions and highlight it as a promising alternative to hypochlorite-based disinfection. The results of this study revealed that OXONE was able to promote significant inactivation of 7 day-old biofilms formed under conditions mimicking DWDS, with a reduction of biofilm culturability and the number of non-damaged cells up to approximately 4 log. The relevance of OXONE was supported by the significant effects on biofilm control and its chemical stability in comparison to the results for chlorine. Moreover, during *S. maltophilia* exposure to OXONE, the formation of reactive species was detected by EPR, demonstrating the presence of singlet oxygen and other free radicals. More information on the toxicological profile of OXONE for long-term exposure via the oral route would help to establish a safe guideline value for routine DW treatment with OXONE. Even though, a possible application of OXONE may be proposed in a first instance for temporary emergency disinfection of DW biofilms.

Environmental implication

Drinking water distribution systems are prone to biofilm formation in the inner walls of pipelines. Biofilms, which can harbour pathogenic microorganisms, are responsible for water quality deterioration and a possible source of hazard human health effects. Besides, the action of conventional hypochlorite-based disinfection is limited by the emergence of microbial tolerance to chlorine and disinfectant decay events. This study explores the use of peroxymonosulphate as an efficient strategy to control drinking water biofilms taking into consideration its chemical stability and mechanism of antimicrobial action in environmental-related conditions. The findings demonstrate the potential of peroxymonosulphateas an alternative to chlorine disinfection for biofilm control in drinkingwater distribution systems

CRediT authorship contribution statement

Isabel Maria Oliveira: Conceptualization, Methodology, Validation, Formal analysis, Investigation, Writing – original draft, Funding acquisition. **Inês Bezerra Gomes:** Writing – review & editing. **Tânia Moniz:** Investigation, Writing – review & editing.**Lúcia Chaves Simões:** Writing – review & editing, Supervision. **Maria Rangel:** Conceptualization, Methodology, Resources, Writing – review & editing, Supervision.**Manuel Simões:** Conceptualization, Methodology, Resources, Writing – review & editing, Supervision, Project administration, Funding acquisition.

Declaration of Competing Interest

The authors declare that they have no known competing financial interests or personal relationships that could have appeared to influence the work reported in this paper.

Data availability

Data will be made available on request.

Acknowledgements

This work was financially supported by: LA/P/0045/2020 (ALiCE), UIDB/00511/2020, UIDP/00511/2020 (LEPABE), UIDB/BIO/04469/2020 (CEB), LA/P/0029/2020 (LABBELS), PRESAGE - Aquatic/0007/2020, UIDB/50006/2020, UIDP/50006/2020, funded by national funds through FCT/MCTES (PIDDAC); Project Germirrad – POCI-01–0247-FEDER-072237 supported by COMPETE2020 – Programa Operacional Competitividade e Internacionalização (POCI) and FCT/MCTES (PIDDAC); HealthyWaters – NORTE-01–0145-FEDER-000069 funded by NORTE 2020 – Norte Portugal Regional Operational Programme under the PORTUGAL 2020 Partnership Agreement, through the European Regional Development Fund (ERDF); FCT PhD grant awarded to Isabel Maria Oliveira (SFRH/BD/138117/2018) and the Inês B. Gomes'

contract supported by FCT (2022.06488. CEECIND).

References

[1] U.N. General Assembly, 2010. A/RES/64/292 Resolution adopted by General Assembly on 28 July 2010. 64/292. The human right to water and sanitation. ⟨https://documents-dds-ny.un.org/doc/UNDOC/GEN/N09/479/35/PDF/N0947935.pdf?OpenElement⟩ (accessed 5.2.23).

[2] WHO/UNICEF, (2021). Progress on household drinking water, sanitation and hygiene 2000–2020: five years into the SDGs. Geneva: World Health Organization (WHO) and the United Nations Children's Fund (UNICEF). Licence: CC BY-NC-SA 3.0 IGO.

[3] Liu, S., Gunawan, C., Barraud, N., Rice, S.A., Harry, E.J., Amal, R., 2016. Understanding, monitoring, and controlling biofilm growth in drinking water distribution systems. Environ Sci Technol 50, 8954–8976. https://doi.org/10.1021/acs.est.6b00835.

[4] Simões, L.C., Simões, M., 2013. Biofilms in drinking water: problems and solutions. RSC Adv 3, 2520–2533. https://doi.org/10.1039/c2ra22243d.

[5] Mezule, L., Denisova, V., Briedis, A., Reimanis, M., Ozolins, J., Juhna, T., 2015. Disinfection effect of electrochemically generated chlorine on surface associated *Escherichia coli* in a drinking water system. Desalin Water Treat 53, 3704–3710. https://doi.org/10.1080/19443994.2013.873742.

[6] Rand, J.L., Sharafimasooleh, M., Walsh, M.E., 2013. Effect of water hardness and pipe material on enhanced disinfection with UV light and chlorine. J Water Supply Res Technol 62, 426–432. https://doi.org/10.2166/aqua.2013.060.

[7] Wang, H.B., Hu, C., Hu, X.X., 2014. Effects of combined UV and chlorine disinfection on corrosion and water quality within reclaimed water distribution systems. Eng Fail Anal 39, 12–20. https://doi.org/10.1016/j.engfailanal.2014.01.009.

[8] Liu, L., Xing, X., Hu, C., Wang, H., Lyu, L., 2019. Effect of sequential UV/free chlorine disinfection on opportunistic pathogens and microbial community structure in simulated drinking water distribution systems. Chemosphere 219, 971–980. https://doi.org/10.1016/j.chemosphere.2018.12.067.

[9] Liu, L.Z., Xing, X.C., Hu, C., Wang, H.B., 2019. O_3-BAC-Cl_2: a multi-barrier process controlling the regrowth of opportunistic waterborne pathogens in drinking water distribution systems. J Environ Sci 76, 142–153. https://doi.org/10.1016/j.jes.2018.04.017.

[10] Wang, H., Hu, C., Zhang, S., Liu, L., Xing, X., 2018. Effects of O_3/Cl_2 disinfection on corrosion and opportunistic pathogens growth in drinking water distribution systems. J Environ Sci 73, 38–46. https://doi.org/10.1016/j.jes.2018.01.009.

[11] World Health Organization (WHO), (2022). Guidelines for drinking-water quality: fourth edition incorporating the first and second addenda. Licence: CC BY-NC-SA 3.0 IGO.

[12] Xue, Z., Seo, Y., 2013. Impact of chlorine disinfection on redistribution of cell clusters from biofilms. Environ Sci Technol 47, 1365–1372. https://doi.org/10.1021/es304113e.

[13] Khan, S., Beattie, T.K., Knapp, C.W., 2019. Rapid selection of antimicrobial-resistant bacteria in complex water systems by chlorine and pipe materials. Environ Chem Lett 17, 1367–1373. https://doi.org/10.1007/s10311-019-00867-z.

[14] Soto-Giron, M.J., Rodriguez-R, L.M., Luo, C.W., Elk, M., Ryu, H., Hoelle, J., et al., 2016. Biofilms on hospital shower hoses: characterization and implications for nosocomial infections. Appl Environ Microbiol 82, 2872–2883. https://doi.org/10.1128/AEM.03529-15.

[15] García-Ávila, F., Sánchez-Alvarracín, C., Cadme-Galabay, M., Conchado-Martínez, J., García-Mera, G., Zhindón-Arévalo, C., 2020. Relationship between chlorine decay and temperature in the drinking water. MethodsX 7, 101002. https://doi.org/10.1016/j.mex.2020.101002.

[16] Gomes, I.B., Simões, L.C., Simões, M., 2020. Influence of surface copper content on *Stenotrophomonas maltophilia* biofilm control using chlorine and mechanical stress. Biofouling 36, 1–13. https://doi.org/10.1080/08927014.2019.1708334.

[17] Onyutha, C., Kwio-Tamale, J.C., 2022. Modelling chlorine residuals in drinking water: a review. Int J Environ Sci Technol 19, 11613–11630. https://doi.org/10.1007/s13762-022-03924-3.

[18] Kali, S., Khan, M., Ghaffar, M.S., Rasheed, S., Waseem, A., Iqbal, M.M., et al., 2021. Occurrence, influencing factors, toxicity, regulations, and abatement approaches for disinfection by-products in chlorinated drinking water: a comprehensive review. Environ Pollut 281, 116950. https://doi.org/10.1016/j.envpol.2021.116950.

[19] Li, X.-F., Mitch, W.A., 2018. Drinking water disinfection byproducts (DBPs) and human health effects: multidisciplinary challenges and opportunities. Environ Sci Technol 52, 1681–1689. https://doi.org/10.1021/acs.est.7b05440.

[20] European Chemicals Agency (ECHA), (2023). Pentapotassium bis (peroxymonosulphate) bis(sulphate) factsheet. ⟨https://echa.europa.eu/pt/information-on-chemicals/biocidal-active-substances/-/disas/factsheet/1339/PT05⟩ (accessed 2.20.23).

[21] Ghanbari, F., Moradi, M., 2017. Application of peroxymonosulfate and its activation methods for degradation of environmental organic pollutants: review. Chem Eng J 310, 41–62. https://doi.org/10.1016/j.cej.2016.10.064.

[22] Lee, J., Von Gunten, U., Kim, J.H., 2020. Persulfate-based advanced oxidation: critical assessment of opportunities and roadblocks. Environ Sci Technol 54, 3064–3081. https://doi.org/10.1021/acs.est.9b07082.

[23] Gao, P., Yan, S., Tian, X., Nie, Y., Wang, Y., Deng, Y., et al., 2022. Identification and manipulation of active centers on perovskites to enhance catalysis of peroxymonosulfate for degradation of emerging pollutants in water. J Hazard Mater 424, 127384. https://doi.org/10.1016/j.jhazmat.2021.127384.

[24] Zhao, X., Jia, X., Li, H., Zhang, H., Zhou, X., Zhou, Y., et al., 2022. Efficient degradation of health-threatening organic pollutants in water by atomically dispersed cobalt-activated peroxymonosulfate. Chem Eng J 450, 138098. https://doi.org/10.1016/j.cej.2022.138098.

[25] Wang, Linlin, Wang, Liang, Shi, Y., Zhu, J., Zhao, B., Zhang, Z., et al., 2022. Fabrication of Co_3O_4-Bi_2O_3-Ti catalytic membrane for efficient degradation of organic pollutants in water by peroxymonosulfate activation. J Colloid Interface Sci 607, 451–461. https://doi.org/10.1016/j.jcis.2021.08.086.

[26] Cai, C., Liu, Y., Xu, R., Zhou, J., Zhang, J., Chen, Y., et al., 2023. Bicarbonate enhanced heterogeneous activation of peroxymonosulfate by copper ferrite nanoparticles for the efficient degradation of refractory organic contaminants in water. Chemosphere 312, 137285. https://doi.org/10.1016/j.chemosphere.2022.137285.

[27] Wang, Y., Tong, Y., Chen, D., Zhou, T., Zhang, Q., Zou, J.-P., 2023. Activation of peroxymonosulfate by g-C_3N_4/ε-MnO_2 microspheres for nonradical pathway degradation of organic pollutants in water: catalytic mechanism and degradation path. Chem Eng J 459, 141643. https://doi.org/10.1016/j.cej.2023.141643.

[28] Hu, Y., Chen, D., Wang, S., Zhang, R., Wang, Y., Liu, M., 2022. Activation of peroxymonosulfate by nitrogen-doped porous carbon for efficient degradation of organic pollutants in water: performance and mechanism. Sep Purif Technol 280, 119791. https://doi.org/10.1016/j.seppur.2021.119791.

[29] Gomes, I.B., Madureira, D., Simoes, L.C., Simoes, M., 2019. The effects of pharmaceutical and personal care products on the behavior of *Burkholderia cepacia* isolated from drinking water. Int Biodeterior Biodegrad 141, 87–93. https://doi.org/10.1016/j.ibiod.2018.03.018.

[30] Gomes, I.B., Maillard, J.-Y., Simões, L.C., Simões, M., 2020. Emerging contaminants affect the microbiome of water systems-strategies for their mitigation. npj Clean Water 3, 39. https://doi.org/10.1038/s41545-020-00086-y.

[31] Pereira, A.R., Gomes, I.B., Simões, M., 2023. Impact of parabens on drinking water bacteria and their biofilms: the role of exposure time and substrate materials. J Environ Manag 332, 117413. https://doi.org/10.1016/j.jenvman.2023.117413.

[32] Duan, X., Sun, H., Kang, J., Wang, Y., Indrawirawan, S., Wang, S., 2015. Insights into heterogeneous catalysis of persulfate activation on dimensional-structured nanocarbons. ACS Catal 5, 4629–4636. https://doi.org/10.1021/acscatal.5b00774.

[33] Lee, Y., Lee, S., Cui, M., Ren, Y., Park, B., Ma, J., et al., 2021. Activation of peroxodisulfate and peroxymonosulfate by ultrasound with different frequencies: impact on ibuprofen removal efficiency, cost estimation and energy analysis. Chem Eng J 413, 127487. https://doi.org/10.1016/j.cej.2020.127487.

[34] Wacławek, S., Lutze, H.V., Grübel, K., Padil, V.V.T., Černík, M., Dionysiou, D.D., 2017. Chemistry of persulfates in water and wastewater treatment: A review. Chem Eng J 330, 44–62. https://doi.org/10.1016/j.cej.2017.07.132.

[35] Anipsitakis, G.P., Tufano, T.P., Dionysiou, D.D., 2008. Chemical and microbial decontamination of pool water using activated potassium peroxymonosulfate. Water Res 42, 2899–2910. https://doi.org/10.1016/j.watres.2008.03.002.

[36] Delcomyn, C.A., Bushway, K.E., Henley, M.V., 2006. Inactivation of biological agents using neutral oxone-chloride solutions. Environ Sci Technol 40, 2759–2764. https://doi.org/10.1021/es052146+.

[37] Lee, H.-J., Kim, H.-E., Kim, M.S., de Lannoy, C.-F., Lee, C., 2020. Inactivation of bacterial planktonic cells and biofilms by Cu(II)-activated peroxymonosulfate in the presence of chloride ion. Chem Eng J 380, 122468. https://doi.org/10.1016/j.cej.2019.122468.

[38] Wen, G., Zhao, D., Xu, X., Chen, Z., Huang, T., Ma, J., 2019. Inactivation of fungi from four typical genera in groundwater using PMS/Cl^- system: Efficacy, kinetics and mechanisms. Chem Eng J 357, 567–578. https://doi.org/10.1016/j.cej.2018.09.195.

[39] Oliveira, I.M., Gomes, I.B., Simões, L.C., Simões, M., 2022. Chlorinated cyanurates and potassium salt of peroxymonosulphate as antimicrobial and antibiofilm agents for drinking water disinfection. Sci Total Environ 811. https://doi.org/10.1016/j.scitotenv.2021.152355.

[40] Gomes, I.B., Simões, M., Simões, L.C., 2014. An overview on the reactors to study drinking water biofilms. Water Res 62, 63–87. https://doi.org/10.1016/j.watres.2014.05.039.

[41] Cervia, J.S., Ortolano, G.A., Canonica, F.P., 2008. Hospital tap water as a source of *Stenotrophomonas maltophilia* infection. Clin Infect Dis Publ Infect Dis Soc Am. https://doi.org/10.1086/587180.

[42] Gröschel, M.I., Meehan, C.J., Barilar, I., Diricks, M., Gonzaga, A., Steglich, M., et al., 2020. The phylogenetic landscape and nosocomial spread of the multidrug-resistant opportunist *Stenotrophomonas maltophilia*. Nat Commun 11, 2044. https://doi.org/10.1038/s41467-020-15123-0.

[43] Maes, S., Vackier, T., Huu, S.N., Heyndrickx, M., Steenackers, H., Sampers, I., et al., 2019. Occurrence and characterisation of biofilms in drinking water systems of broiler houses. BMC Microbiol 19. https://doi.org/10.1186/s12866-019-1451-5.

[44] Menetrey, Q., Sorlin, P., Jumas-Bilak, E., Chiron, R., Dupont, C., Marchandin, H., 2021. *Achromobacter xylosoxidans* and *Stenotrophomonas maltophilia*: emerging pathogens well-armed for life in the cystic fibrosis patients' lung. Genes (Basel). https://doi.org/10.3390/genes12050610.

[45] Zainulabid, U.A., Siew, S.W., Musa, S.M., Soffian, S.N., Periyasamy, P., Ahmad, H. F., 2023. Whole-genome sequence of a *Stenotrophomonas maltophilia* isolate from tap water in an intensive care unit. Microbiol Resour Announc 12 (2), 1. https://doi.org/10.1128/mra.00995-22.

[46] Guyot, A., Turton, J.F., Garner, D., 2013. Outbreak of *Stenotrophomonas maltophilia* on an intensive care unit. J Hosp Infect 85, 303–307. https://doi.org/10.1016/j.jhin.2013.09.007.

[47] Gomes, I.B., Lemos, M., Mathieu, L., Simoes, M., Simoes, L.C., 2018. The action of chemical and mechanical stresses on single and dual species biofilm removal of

drinking water bacteria. Sci Total Environ 631–632, 987–993. https://doi.org/10.1016/j.scitotenv.2018.03.042.
[48] European Chemicals Agency (ECHA), (2020). Article 95 List of active substances and product suppliers. ⟨https://echa.europa.eu/pt/information-on-chemicals/active-substance-suppliers⟩ (accessed 7.30.20).
[49] Meireles, A., Ferreira, C., Melo, L., Simões, M., 2017. Comparative stability and efficacy of selected chlorine-based biocides against *Escherichia coli* in planktonic and biofilm states. Food Res Int 102, 511–518. https://doi.org/10.1016/j.foodres.2017.09.033.
[50] Gomes, I.B., Simões, L.C., Simões, M., 2018. The effects of emerging environmental contaminants on *Stenotrophomonas maltophilia* isolated from drinking water in planktonic and sessile states. Sci Total Environ 643, 1348–1356. https://doi.org/10.1016/j.scitotenv.2018.06.263.
[51] Lemos, M., Mergulhão, F., Melo, L., Simões, M., 2015. The effect of shear stress on the formation and removal of *Bacillus cereus* biofilms. Food Bioprod Process 93, 242–248. https://doi.org/10.1016/j.fbp.2014.09.005.
[52] Simões, L.C., Simões, M., Oliveira, R., Vieira, M.J., 2007. Potential of the adhesion of bacteria isolated from drinking water to materials. J Basic Microbiol 47, 174–183. https://doi.org/10.1002/jobm.200610224.
[53] Learbuch, K.L.G., Smidt, H., van der Wielen, P.W.J.J., 2021. Influence of pipe materials on the microbial community in unchlorinated drinking water and biofilm. Water Res 194, 116922. https://doi.org/10.1016/j.watres.2021.116922.
[54] Fu, Y., Peng, H., Liu, J., Nguyen, T.H., Hashmi, M.Z., Shen, C., 2021. Occurrence and quantification of culturable and viable but non-culturable (VBNC) pathogens in biofilm on different pipes from a metropolitan drinking water distribution system. Sci Total Environ 764, 142851. https://doi.org/10.1016/j.scitotenv.2020.142851.
[55] Husband, P.S., Boxall, J.B., 2011. Asset deterioration and discolouration in water distribution systems. Water Res 45, 113–124. https://doi.org/10.1016/j.watres.2010.08.021.
[56] Ragain, L., Masters, S., Bartrand, T.A., Clancy, J.L., Whelton, A.J., 2019. Analysis of building plumbing system flushing practices and communications. J Water Health 17, 196–203. https://doi.org/10.2166/wh.2019.024.
[57] Simões, M., Pereira, M.O., Vieira, M.J., 2005. Effect of mechanical stress on biofilms challenged by different chemicals. Water Res 39, 5142–5152. https://doi.org/10.1016/j.watres.2005.09.028.
[58] Frølund, B., Palmgren, R., Keiding, K., Nielsen, P.H., 1996. Extraction of extracellular polymers from activated sludge using a cation exchange resin. Water Res 30, 1749–1758. https://doi.org/10.1016/0043-1354(95)00323-1.
[59] Lowry, O.H., Rosebrough, N.J., Farr, A.L., Randall, R.J., 1951. Protein measurement with the folin phenol reagent. J Biol Chem 193, 265–275. https://doi.org/10.1016/S0021-9258(19)52451-6.
[60] Peterson, G.L., 1977. A simplification of the protein assay method of Lowry et al. which is more generally applicable. Anal Biochem 83, 346–356. https://doi.org/10.1016/0003-2697(77)90043-4.
[61] Dubois, M., Gilles, K., Hamilton, J.K., Rebers, P.A., Smith, F., 1951. A colorimetric method for the determination of sugars. Nature 168, 167. https://doi.org/10.1038/168167a0.
[62] European Standard, (1997). Chemical disinfectants and antiseptics - Quantitative suspension test for the evaluation of bactericidal activity of chemical disinfectants and antiseptics used in food, industrial, domestic, and institutional areas - Test method and requirements (phase 2, step 1).
[63] Zou, J., Huang, Y., Zhu, L., Cui, Z., Yuan, B., 2019. Multi-wavelength spectrophotometric measurement of persulfates using 2,2′-azino-bis(3-ethylbenzothiazoline-6-sulfonate) (ABTS) as indicator. Spectrochim Acta Part A Mol Biomol Spectrosc 216, 214–220. https://doi.org/10.1016/j.saa.2019.03.019.
[64] Rebelo, S.L.H., Moniz, T., Medforth, C.J., de Castro, B., Rangel, M., 2019. EPR spin trapping studies of H_2O_2 activation in metaloporphyrin catalyzed oxygenation reactions: insights on the biomimetic mechanism. Mol Catal 475, 110500. https://doi.org/10.1016/j.mcat.2019.110500.
[65] Li, W., Tan, Q., Zhou, W., Chen, J., Li, Y., Wang, F., et al., 2020. Impact of substrate material and chlorine/chloramine on the composition and function of a young biofilm microbial community as revealed by high-throughput 16S rRNA sequencing. Chemosphere 242, 125310. https://doi.org/10.1016/j.chemosphere.2019.125310.
[66] Sharafimasooleh, M., Rand, J.L., Walsh, M.E., 2016. Effect of high chloride concentrations on microbial regrowth in drinking water distribution systems. J Environ Eng 142. https://doi.org/10.1061/(ASCE)EE.1943-7870.0001027.
[67] Xing, X.C., Wang, H.B., Hu, C., Liu, L.Z., 2018. Effects of phosphate-enhanced ozone/biofiltration on formation of disinfection byproducts and occurrence of opportunistic pathogens in drinking water distribution systems. Water Res 139, 168–176. https://doi.org/10.1016/j.watres.2018.03.073.
[68] Yan, X., Lin, T., Wang, X., Zhang, S., Zhou, K., 2022. Effects of pipe materials on the characteristic recognition, disinfection byproduct formation, and toxicity risk of pipe wall biofilms during chlorination in water supply pipelines. Water Res 210, 117980. https://doi.org/10.1016/j.watres.2021.117980.
[69] Mathieu, L., Bertrand, I., Abe, Y., Angel, E., Block, J.C., Skali-Lami, S., et al., 2014. Drinking water biofilm cohesiveness changes under chlorination or hydrodynamic stress. Water Res 55, 175–184. https://doi.org/10.1016/j.watres.2014.01.054.
[70] Shen, Y., Huang, C., Monroy, G.L., Janjaroen, D., Derlon, N., Lin, J., et al., 2016. Response of simulated drinking water biofilm mechanical and structural properties to long-term disinfectant exposure. Environ Sci Technol 50, 1779–1787. https://doi.org/10.1021/acs.est.5b04653.
[71] Assaidi, A., Ellouali, M., Latrache, H., Zahir, H., Karoumi, A., Mliji, E.M., 2020. Chlorine disinfection against *Legionella pneumophila* biofilms. J Water Sanit Hyg Dev 10, 885–893. https://doi.org/10.2166/washdev.2020.151.
[72] Hemdan, B., Azab El-Liethy, M., El-Taweel, G.E., 2020. The destruction of *Escherichia coli* adhered to pipe surfaces in a model drinking water distribution system via various antibiofilm agents. Water Environ Res 92, 2155–2167. https://doi.org/10.1002/wer.1388.
[73] Feng, K., Li, Q., 2022. Chloride-enhanced removal of ammonia nitrogen and organic matter from landfill leachate by a microwave/peroxymonosulfate system. Catalysts. https://doi.org/10.3390/catal12101078.
[74] Brown, D., Bridgeman, J., West, J.R., 2011. Predicting chlorine decay and THM formation in water supply systems. Rev Environ Sci Bio Technol 10, 79–99. https://doi.org/10.1007/s11157-011-9229-8.
[75] Kiéné, L., Lu, W., Lévi, Y., 1998. Relative importance of the phenomena responsible for chlorine decay in drinking water distribution systems. Water Sci Technol 38, 219–227. https://doi.org/10.1016/S0273-1223(98)00583-6.
[76] Shi, X., Clark, G.G., Huang, C., Nguyen, T.H., Yuan, B., 2022. Chlorine decay and disinfection by-products formation during chlorination of biofilms formed with simulated drinking water containing corrosion inhibitors. Sci Total Environ 815, 152763. https://doi.org/10.1016/j.scitotenv.2021.152763.
[77] Tonev, R., Dimova, G., 2020. Investigation of chlorine wall decay in an old, decommissioned metallic pipe using a pipe section reactor. Water Supply 20, 953–962. https://doi.org/10.2166/ws.2020.017.
[78] Agudelo-Vera, C., Avvedimento, S., Boxall, J., Creaco, E., de Kater, H., Di Nardo, A., et al., 2020. Drinking water temperature around the globe: understanding, policies, challenges and opportunities. Water 12, 1049. https://doi.org/10.3390/w12041049.
[79] Deborde, M., von Gunten, U., 2008. Reactions of chlorine with inorganic and organic compounds during water treatment—kinetics and mechanisms: a critical review. Water Res 42, 13–51. https://doi.org/10.1016/j.watres.2007.07.025.
[80] BusinessAnalytiq, (2023). Chlorine price index July 2023 and outlook. ⟨https://businessanalytiq.com/procurementanalytics/index/chlorine-price-index/⟩ (accessed 7.31.23).
[81] Dore, M.H.I., Singh, R.G., Achari, G., Moghadam, A.K., 2013. Cost scenarios for small drinking water treatment technologies. Desalin Water Treat 51, 3628–3638. https://doi.org/10.1080/19443994.2012.751148.
[82] Moghadam, A.K., Dore, M., 2012. Cost and efficacy of water disinfection practices: evidence from Canada. Rev Econ Anal 4, 209–223. https://doi.org/10.15353/rea.v4i2.1384.
[83] Liu, Y., Wang, L., Dong, Y., Peng, W., Fu, Y., Li, Q., et al., 2021. Current analytical methods for the determination of persulfate in aqueous solutions: a historical review. Chem Eng J 416. https://doi.org/10.1016/j.cej.2021.129143.
[84] Lopes, J.C., Moniz, T., Sampaio, M.J., Silva, C.G., Rangel, M., Faria, J.L., 2023. Efficient synthesis of imines using carbon nitride as photocatalyst. Catal Today 418, 114045. https://doi.org/10.1016/j.cattod.2023.114045.
[85] Miyaji, A., Gabe, Y., Kohno, M., Baba, T., 2017. Generation of hydroxyl radicals and singlet oxygen during oxidation of rhododendrol and rhododendrol-catechol. J Clin Biochem Nutr 60, 86–92. https://doi.org/10.3164/jcbn.16-38.
[86] Qi, C., Liu, X., Ma, J., Lin, C., Li, X., Zhang, H., 2016. Activation of peroxymonosulfate by base: implications for the degradation of organic pollutants. Chemosphere 151, 280–288. https://doi.org/10.1016/j.chemosphere.2016.02.089.
[87] Tian, X., Sun, Y., Fan, S., Boudreau, M.D., Chen, C., Ge, C., et al., 2019. Photogenerated charge carriers in molybdenum disulfide quantum dots with enhanced antibacterial activity. ACS Appl Mater Interfaces 11, 4858–4866. https://doi.org/10.1021/acsami.8b19958.
[88] Hamblin, M.R., Hasan, T., 2004. Photodynamic therapy: a new antimicrobial approach to infectious disease. Photochem Photobiol Sci J Eur Photochem Assoc Eur Soc Photobiol 3, 436–450. https://doi.org/10.1039/b311900a.
[89] Lee, J., Mackeyev, Y., Cho, M., Li, D., Kim, J.-H., Wilson, L.J., et al., 2009. Photochemical and antimicrobial properties of novel C60 derivatives in aqueous systems. Environ Sci Technol 43, 6604–6610. https://doi.org/10.1021/es901501k.
[90] Manjón, F., Villén, L., García-Fresnadillo, D., Orellana, G., 2008. On the factors influencing the performance of solar reactors for water disinfection with photosensitized singlet oxygen. Environ Sci Technol 42, 301–307. https://doi.org/10.1021/es071762y.
[91] Redmond, R.W., Gamlin, J.N., 1999. A compilation of singlet oxygen yields from biologically relevant molecules. Photochem Photobiol 70, 391–475.
[92] Qi, H., Huang, Q., Hung, Y.-C., 2018. Efficacy of activated persulfate in inactivating *Escherichia coli* O157:H7 and *Listeria monocytogenes*. Int J Food Microbiol 284, 40–47. https://doi.org/10.1016/j.ijfoodmicro.2018.06.021.
[93] Wordofa, D.N., Walker, S.L., Liu, H., 2017. Sulfate radical-induced disinfection of pathogenic *Escherichia coli* O157:H7 via iron-activated persulfate. Environ Sci Technol Lett 4, 154–160. https://doi.org/10.1021/acs.estlett.7b00035.
[94] Xia, D., Li, Y., Huang, G., Yin, R., An, T., Li, G., et al., 2017. Activation of persulfates by natural magnetic pyrrhotite for water disinfection: efficiency, mechanisms, and stability. Water Res 112, 236–247. https://doi.org/10.1016/j.watres.2017.01.052.
[95] Wei, Z., Villamena, F.A., Weavers, L.K., 2017. Kinetics and mechanism of ultrasonic activation of persulfate: an *in situ* EPR spin trapping study. Environ Sci Technol 51, 3410–3417. https://doi.org/10.1021/acs.est.6b05392.
[96] Sun, P., Tyree, C., Huang, C.-H., 2016. Inactivation of *Escherichia coli*, bacteriophage MS2, and *Bacillus* spores under UV/H_2O_2 and UV/peroxydisulfate advanced disinfection conditions. Environ Sci Technol 50, 4448–4458. https://doi.org/10.1021/acs.est.5b06097.
[97] Gao, L., Guo, Y., Zhan, J., Yu, G., Wang, Y., 2022. Assessment of the validity of the quenching method for evaluating the role of reactive species in pollutant abatement during the persulfate-based process. Water Res 221, 118730. https://doi.org/10.1016/j.watres.2022.118730.